Response to Reviewer 1st – Manuscript gmd-2025-268 "Towards an integrated inventory of anthropogenic emissions for China " by Zhang et al., 2025

We would like to thank the reviewer for the careful reading and suggestions to improve the clarity and quality of the manuscript. Below, we provide a detailed reply to each of the comments (Reviewers' comments/questions in bold black, our reply in black, and new text in the manuscript in blue).

Comment 1. Why does the study rely solely on MEIC for China in all harmonized emission inventories instead of using global inventories? The paper devotes substantial effort to harmonizing emission sectors, VOC speciation, and spatial resolution, but these harmonized datasets are not fully utilized to produce the final emissions inventory. Does MEIC significantly outperform the global inventories in China? I did not see supporting evidence for this in Figures 6–7.

We would like to thank the reviewer for their valuable and insightful comments. In our study, we created our final inventory (CINEI) by combining the harmonized national MEIC inventory for mainland China with the global CEDS inventory for regions surrounding mainland China, as described in the manuscript (referred to as HMEI). CINEI also incorporates additional contributions from global inventories, specifically from the agriculture, shipping, and waste sectors. Furthermore, we applied a localized non-methane volatile organic compound (NMVOC) speciation profile within CINEI. For mainland China, we exclusively use MEIC data across all harmonized emission inventories. This choice is based on the fact that MEIC utilizes the most recent and region-specific data for China, including updated emission factors, detailed activity data (such as power plant locations and population), and current mitigation measures (see Section S2). Our study integrates emission estimates derived using these unique factors for all major sectors into the overarching framework of global inventories. As a result, MEIC emissions often differ in magnitude from those reported by other global inventories.

Following the suggestion of the second reviewer, we have updated Table 2 by adding a column labeled 'Selection Principles'. This new column clarifies the criteria we used to select the main sectors (transportation, industry, power, and residential) from the national MEIC inventory.

To address the second part of the comment (model performance), we have now included detailed model validation metrics in Supplementary Section S13, Figures S27–S28. While some deviations between modeled and observed values (see Figures 6–7) can be attributed to spatial averaging, we have now added the Normalized Mean Bias (NMB) directly to these figures for clarity.

- **Winter (Jan 2017):** The MEIC-based HMEI outperforms all other global inventories for multiple pollutants. For ozone, HMEI achieves the lowest NMB (-26%) compared to HTAP (-52%), CEDS (-33%), CAMS (-40%), and CINEI (-44%). It also shows the lowest Mean Normalized Bias (MNB = 15.6%) and the lowest Mean Normalized Absolute Error (MNAE = 43.1%). For CO, HMEI comes closest to zero NMB (-24%) and performs well for NO_2. Overall, the strong performance of HM_CEDS makes it the optimal choice for wintertime air quality modeling.

- **Summer (July 2017):** During July, HMEI continues to outperform other global emission inventories, especially in predicting NO_2 and CO. For NO_2, HMEI provides the most accurate results, with a normalized mean bias (NMB) of 0.5%, which is closest to zero among all inventories compared to CINEI (2%), CAMS (-21%), CEDS (-21%), and HTAP (113%). It also achieves the lowest mean normalized bias (MNB = 41%) and mean normalized absolute error (MNAE = 32.8%). For CO, HMEI again stands out with the best performance (MNB = 57.6%, NMB = -34%, MNAE = 34.4%) despite the fact that all inventories tend to underestimate concentrations. Ozone predictions using HMEI show moderate overestimation (NMB = 20.0%, MNB = 17.3%) compared to other inventories (CINEI: 14%, CAMS: -31%), likely due to reduced NO_2 in polluted regions, which may enhance ozone formation through increased oxidant availability and OH-VOC reactions.

Despite this challenge with summer ozone, HMEI consistently delivers the most reliable results across multiple pollutants in both winter and summer, making it the best choice for year-round atmospheric chemical modeling.

Changes made in the manuscript:

3rd paragraph in section 3.1 (Line 337-345) in main text: The power sector is the main driver of the decrease in NO_x emissions for China, contributing 49% to the downward trend with a linear reduction of -0.33 Tg yr^{-1}. In the CINEI , emissions from the power and industrial sectors (for NO_x) and the residential sector (for CO) started to decline after peaking in 2013 (see Table S16). This timing aligns with the emission reduction measures implemented, starting with the 12th Five-Year Plan in 2011 (see Text S1). The improved reflection of mitigation actions in the MEIC inventory comes from accounting for factors such as technology adoption and abatement efficiency (see Text S2 and Table S1), such as energy transition to cleaner resources (Yan et al., 2023). Over the study period, the sectors responsible for the largest reductions in CO emissions were industry (60% of the reduction), residential (29%), and transportation (16%). The main contributors to the observed linear declines in CO were industry (39% contribution, -3.6 Tg yr^{-1}), residential (22%, -1.8 Tg yr^{-1}), and power generation (13%, 0.14 Tg yr^{-1}).

2nd paragraph in section 3.4 (Line 456-462) in the main text: Further, we investigate ~~that~~ the comparison of experiments' performance between MEIC-based HMEI and global inventories. Modeling ozone mixing ratio using HMEI in January 2017 achieve the smallest normalized mean bias (NMB = -26%), compared with HTAP (-52%), CEDS (-33%), and CAMS (-40%) (Fig. 7). In July 2017, models using HMEI produced NO_2 and CO bias values (NMB = 0.5% for NO_2, -34% for CO) that are closer to zero than results from global inventories (Fig. 6). Comprehensive analysis using several statistical metrics (NMB, MNB, MNAE, MAE, MFE) consistently demonstrates that HMEI delivers superior overall performance compared to individual global emission inventories (Fig. S27-S28). These comparisons of evaluation metrics suggest that CINEI is based on emissions from the main sectors in the MEIC inventory.

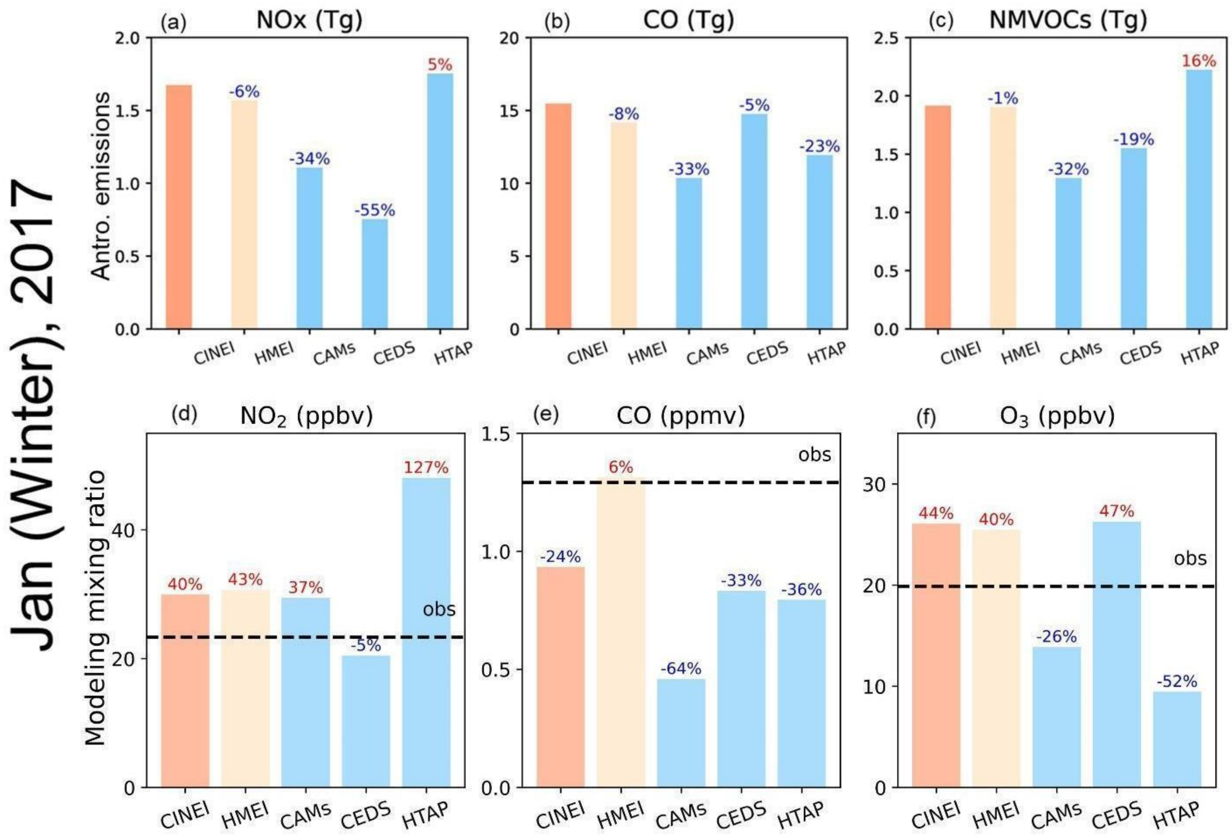

Page 25 in the main text: Figure 6: The top panels (a-c) present total anthropogenic emission differences of ozone precursors (NOx, CO, and NMVOC) for July 2017 between the CINEI, HMEI, CAMS, CEDS, and HTAP inventories using the CINEI integrated emission inventory as a reference. Bottom panels (d-f) show WRF-Chem simulated mixing ratios of O_3, NO_2, and CO for the same month and within the modeling domain (latitudes from 25.5° to 43.6°; longitudes from 103.5° to 127.6°) using the different emission inventories. Individual columns show simulated mean mixing ratios in the model domain for each emission inventory used. The dashed blue lines show average observed mixing ratios calculated using the stations within the specified domain. The numbers shown in the columns represent the normalized mean bias (NMB) against observations for each modeling experiment, as defined in the first line of Table S7. Values in red indicate overestimation, while values in blue indicate underestimation.

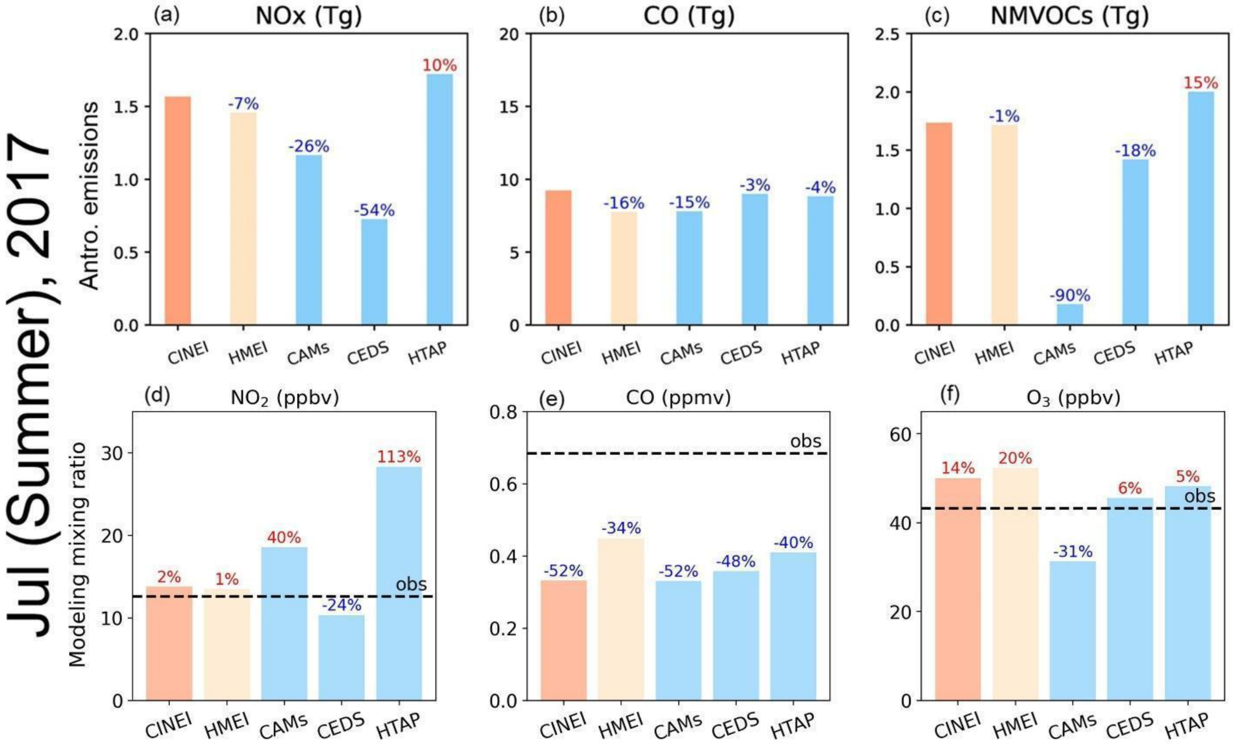

Page 26 in the main text: Figure 7. Same content with Figure 6, but in July 2017.

Comment 2. Additionally, the key distinction between CINEI and MEIC lies in the inclusion of previously missing sources in CINEI, such as agricultural, waste, and marine sectors. While MEIC has been evaluated in previous studies, the current evaluation of CINEI essentially serves to assess the impact of these additional sources. This important insight should be emphasized more clearly and consistently throughout the manuscript.

We thank the reviewer for this suggestion. The key distinction between CINEI and MEIC is indeed the inclusion of agricultural waste and marine (shipping and aviation) sectors, and applying new NMVOC speciated profiles to NMVOC emissions. Our modeling evaluation based on CINEI in this study reveals several differences when compared to previous studies using MEIC and to harmonized MEIC with CEDS inventory (HMEI) in this work. Below, we summarize the improvements associated with these changes in CINEI:

Modeling evaluation:

- In January (Winter), CINEI total emissions over China are (slightly) higher than HMEI: +6% for NO_x, +8% for CO, and +1% for NMVOCs. This increase is due to the inclusion of agricultural, waste, and shipping emissions that are absent in the original MEIC inventory. The additional emissions lead to a small increase in O_3 (less than 1 ppb), along with slight decreases in CO (by 0.4 ppm) and NO_2 (by 1 ppbv) mixing ratios. The improvement for NO_2 is shown by a decrease in normalized mean bias (NMB) from 24% (HMEI) to 22% (CINEI). Other metrics, such as MAE, MNB, and MFE, also support the improvement for NO_2.

- In July (Summer), CINEI shows (slightly) higher emissions compared to HMEI: +7% for NOx, +16% for CO, and +1% for NMVOCs. The added emissions increase O_3 by 3 ppb but lower CO (by 0.17 ppm) and NO_2 (by 2 ppbv). For O_3, the NMB improves from 21% (HMEI) to 12% (CINEI), as supported by additional evaluation metrics.

Impact of additional sectoral emission contributions:

The CINEI inventory includes previously missing sectors for NOx and CO emissions. Based on our results:
- The shipping sector is identified as a key sector for NOx emission in China, because the linear emission change rate of shipping NOx is +0.07 Tg yr^{-1} and it ranks as the 3rd largest contributor to the total trend (21%).
- The aviation sector is also a key sector for NOx emission due to being the 4th contributor to the total trend (3% and +0.01 Tg yr^{-1}).
- Waste CO emission is the 4th largest contributor (13%) to the total trend and has an increasing trend (linear slope: +0.15 Tg yr^{-1}).

4th paragraph in section 3.1 (Line 351-359) in main text (sectoral emission): Ozone precursor emissions from four key sectors not included in the MEIC inventory (shipping, waste, agriculture, and aviation) are included in the CINEI inventory and are identified as key contributors (see Tables S12-15 and Text S8). The shipping sector is a major contributor to NO_x emissions in China, with a linear emission increase of +0.07 Tg yr^{-1} , making it the third-largest driver of the total NO_x trend at 21%. Aviation follows as the fourth-largest contributor to NO_x with 3% (+0.01 Tg yr^{-1}), while waste accounts for the fourth-largest share of the CO trend at 13% and also shows a rising trajectory (+0.15 Tg yr^{-1}, see Table S13). For comparison, NO_x emissions from shipping in the HTAP inventory also display an upward trend of +0.1 Tg yr^{-1} (Table S12), which appears to counteract reductions from the energy sector. In summary, our findings indicate that shipping, waste, aviation, and agriculture are key sectors that influence overall trends, often showing increases where other major sectors have declined.

3rd paragraph in section 3.2 Line 398-404 in main text (NMVOC emission): All of the major NMVOC species identified by CINEI show increasing trends within the sectors added from global inventories, namely agriculture, shipping, aviation, and waste. For example, total NMVOC emissions from the agriculture sector are slightly rising by +0.003 Tg yr^{-1}. Key speciated NMVOC emissions from these four sectors, such as ethene (which contributes 8% to total OFP) and formaldehyde (5%), also show notable increases. To effectively reduce ozone levels, mitigation strategies should target not only highly reactive species like m/p-xylene, toluene, and propene from industrial sources, but also address emissions from sectors like agriculture and aviation that are often overlooked in national inventories.

The last paragraph in section 3.2 Line 418-426 in the main text (NMVOC speciation): When compared to the national inventory (MEIC, with the same ratio as the harmonized inventories), the ethane-to-acetylene and propene-to-acetylene ratios in CINEI are closer to the observed ratios (Fig. S17). These findings may be linked to two factors. First, the ethane-to-acetylene ratio in CINEI is higher than the MEIC ratio resulting from the incorporation of missing sectors (agriculture, aviation, ships, and waste), which contribute 13% to the total annual average emission and are richer in ethane. Second, the propene-to-acetylene ratio in CINEI is lower than the MEIC ratio despite a 3% additional contribution from these missing sectors. This may be due to the speciated profile used in CINEI (Mo et al., 2018), which attributes a smaller share of emissions to diesel vehicles (mainly emitting alkenes) and a larger share to gasoline vehicles (mainly emitting alkanes) (Table S20). These findings suggest that using local NMVOC speciated profiles can better capture changes caused by current energy transitions and evolving consumption patterns (Yan et al., 2021).

3rd paragraph in section 3.4 (Line 473-477) in main text (Modeling evaluation): The differences between the two emission inventories can be attributed to the inclusion of shipping, waste, and aviation emissions, as well as updated NMVOC speciation in the CINEI dataset. Accounting for these sectors results in a modest increase in total emissions (less than 10%) in CINEI. This change leads to improved model performance, as shown by a reduction in the normalized mean bias (NMB) for ozone in summer (from 21% with HMEI to 12% with CINEI) and for NO_2 in winter (from 24% with HMEI to 22% with CINEI).

Comment 3. Section 3.2 and Figure 4a: What causes the large year-to-year fluctuations in ozone formation potentials (OFPs)?

The ozone formation potential (OFP) measures how much each volatile organic compound (VOC) can contribute to ozone creation. It is expressed in Tg of ozone (Tg-O_3) yr^{-1}. OFP for each VOC species is calculated by multiplying that species' emissions by its maximum incremental reactivity (MIR). Year-to-year changes in OFP depend, therefore, on (1) the reactivity of different NMVOC species, as measured by their MIR (Carter, 2015), and (2) each species' share of total OFP. Trends in emissions of individual NMVOCs are closely linked to their relative abundance and the dominant emitting sectors. Figure 3 displays OFP and emission trends for the major (top 20) VOC species contributing to total OFP from 2008 to 2020.

China's total NMVOC emissions and OFPs, summing all species, increased from 2008 to 2020, with linear trends of 0.2 Tg yr^{-1} for emissions and 1.1 Tg-O_3 yr^{-1} for OFP (Figure S14). Fourteen of the top 20 species (70% contribution of total emission) showed increasing trends and now make up large portions of OFP, including m/p-xylene (18% of OFP, 0.04 Tg yr^{-1}), propene (18%, 0.2 Tg yr^{-1}), and toluene (10%, 0.03 Tg yr^{-1}). The main sources driving this increase are industrial activities such as industrial painting, iron and steel manufacturing, and architectural coatings (Figure S12).

Some sources like aviation, shipping, and waste, though lower in emissions, also contribute to the overall upward trend. Small decreasing trends can be found in species including i-pentane (-0.005 Tg yr^{-1}), formaldehyde (-0.004 Tg yr^{-1}) and trans-2-butene (-0.002 Tg yr^{-1}). The residential and transportation sectors lead the decreasing trends, but fail to offset the emission increase by the other sectors in the study period. Above all, OFPs increase is driven by high-reactive species like m/p-xylene, toluene, and propene from industrial sources, and slightly from the missing sources (aviation and shipping, etc) by national inventory (MEIC).

3rd paragraph in section 3.2 (Line 389-398) in main text: Total NMVOC emissions and OFPs in China, showed an overall increasing trend from 2008 to 2020, with linear slopes of 0.2 Tg yr^{-1} (emission) and 1.1 Tg-O_3 yr^{-1} (OFPs), as shown in Fig. S14. Fourteen of the top 20 species exhibited increasing trends and contributed significantly to OFPs, including m/p-xylene (18% OFP contribution and 0.04 Tg-O_3 yr^{-1}), propene (18% and 0.2 Tg-O_3 yr^{-1}), and toluene (10% and 0.03 Tg-O_3 yr^{-1}) (Fig. S15 and Fig. S16). The primary driver for this increase was the industrial sector, particularly processes like industrial painting, iron and steel production, and architectural coating (Fig. S12). To mitigate ozone formation, targeted strategies should focus on industrial emission controls for high-OFP species, particularly aromatics like xylenes and toluene, while continuing to strengthen transportation and residential emission reductions. Additionally, since formaldehyde and several alkenes showed decreasing trends, policies should maintain these reductions while preventing industrial sector growth from overwhelming the overall mitigation efforts through stricter industrial VOC controls and cleaner production technologies.

The last paragraph in section S10 (Line 276-281) in SI: Based on the VOC emissions analysis from 2008-2020, the overall mean increase in OFP, of 1.3% annually, was primarily driven by significant growth in industrial emissions, which increased by 3.9% yr^{-1} across most VOC species. This industrial growth more than compensated for the decreasing trends in transportation (-3.3% annually) and residential (-2.2% annually) sectors. The species contributing most to ozone formation, m/p-xylene (17.7% of total OFP), propene (16.7%), and toluene (10.0%), all showed increasing industrial emissions despite reductions from other sectors (Figures S15 and S16).

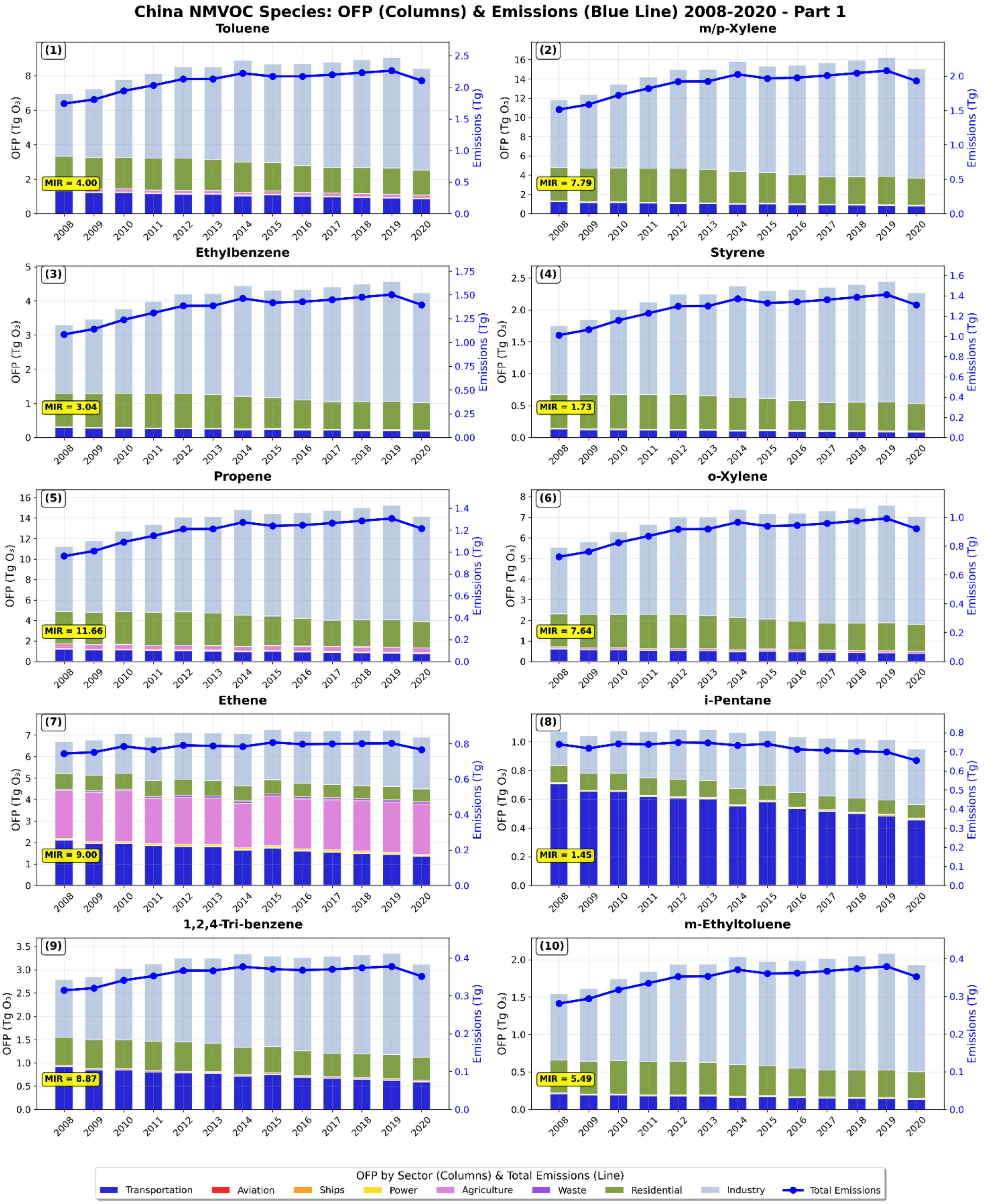

Figure 15. Year-to-year CINEI Ozone formation potentials (OFPs, in columns, unit: Tg-O_3) distinguishing contributions from each sector (see figure legend) and total emission (blue line with dots, unit: Tg) for the TOP-20 important NMVOC species in China from 2008 to 2020. The colors of the columns denote sectors' contribution to OFP.

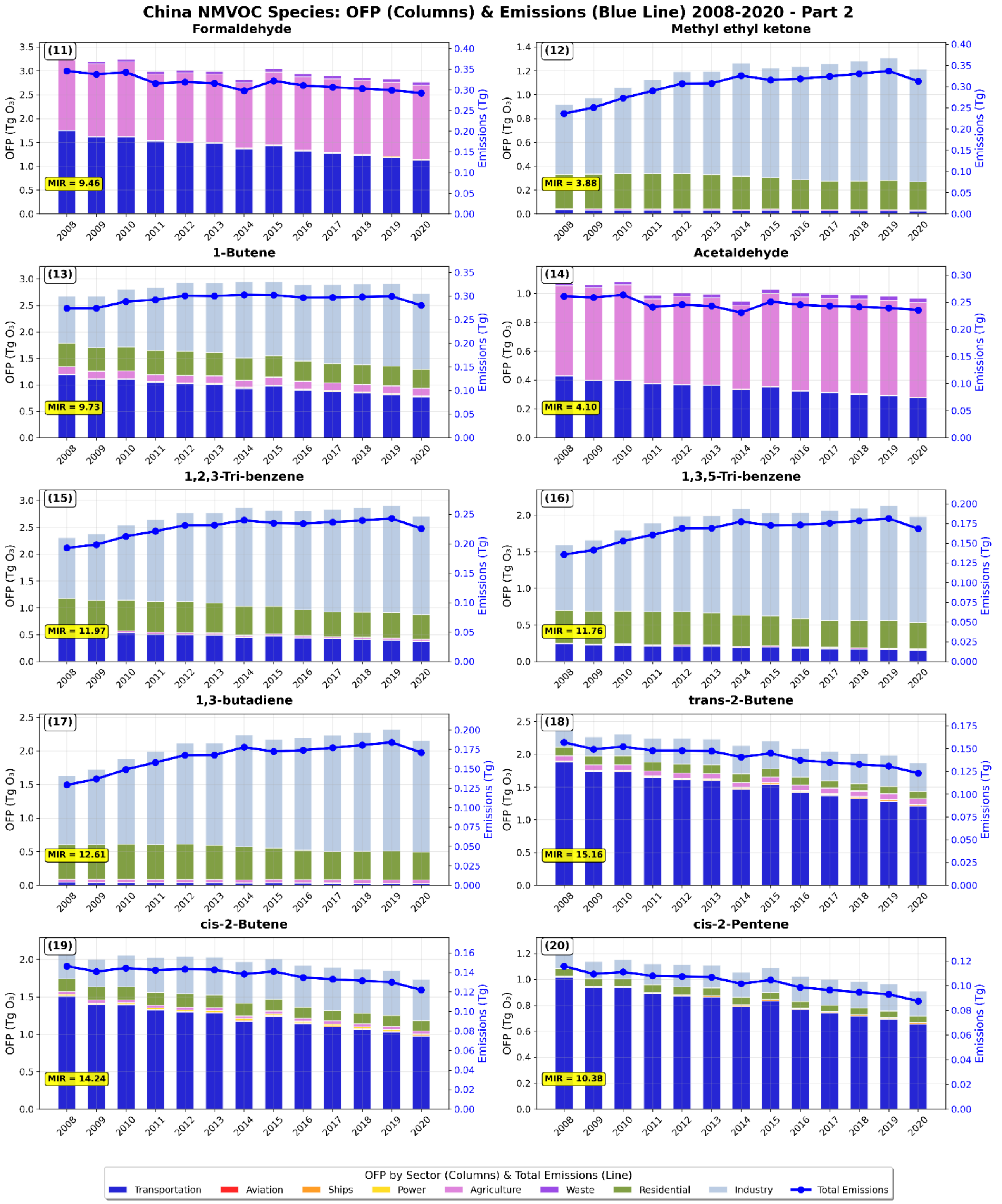

Figure 16. Year-to-year CINEI Ozone formation potentials (OFPs, in columns, unit: Tg-O_3) distinguishing contributions from each sector (see figure legend) and total emissions (blue line with dots, unit: Tg) for the TOP-20 important NMVOC species in China from 2008 to 2020. The colors of the columns denote sectors' contribution to OFP.

Comment 4. How are VOC emissions from volatile chemical products (VCPs) treated in the CINEI inventory?

VCPs represent a specific emission source sector that includes products such as pesticides, coatings, printing inks, adhesives, cleaning agents, and personal care products (McDonald et al., 2018; Seltzer et al., 2021). All of these sources contribute to emissions through evaporation processes. In our approach, we incorporate emissions data for the main sectors from the original MEIC dataset. MEIC classifies VCP emissions into industrial, residential, and agricultural sectors, with examples such as industrial painting, architectural coatings, and printing and dyeing. For transportation, MEIC includes emissions from petrol and diesel vehicles, accounting for both exhaust and evaporation processes.

In CINEI, we categorize VOC emissions from VCPs in two ways: by emission sector and by VOC speciation source profile. First, we obtained total NMVOC emissions from national and global inventories for relevant sectoral emissions. Then, we map emitting sectors to the source profile categorization and use source profile scores to calculate emissions for each species. Finally, we grouped similar species into the MOZART model species.

3rd paragraph Section 2.2 (Line 163-167) in the main text: Emissions from by-product industrial processes include emissions from solvent volatilization, cement, iron and steel production, fugitive emissions, refinery emissions and other fuel-related emissions. This sector also covers emissions from volatile chemical products (VCPs) such as petrochemical products, coatings, and printing inks. These sources emit~~s~~ high-reactivity species such as m/p-xylene, propene, and toluene, which are important contributors to ozone formation.

The last paragraph Section 4 (Line 551) in the main text:
The new version of CINEI will incorporate additional emerging sources, such as new volatile chemical products (VCPs), including the production of personal care products in industry and the use of pesticides in agriculture (Seltzer et al., 2021; Cai et al., 2023).

Reference

Seltzer, K. M., Pennington, E., Rao, V., Murphy, B. N., Strum, M., Isaacs, K. K., and Pye, H. O. T.: Reactive organic carbon emissions from volatile chemical products, Atmospheric Chemistry and Physics, 21, 5079–5100, https://doi.org/10.5194/acp-21-5079-2021, 2021.

McDonald, B. C., de Gouw, J. A., Gilman, J. B., Jathar, S. H., Akherati, A., Cappa, C. D., Jimenez, J. L., Lee-Taylor, J., Hayes, P. L., McKeen, S. A., Cui, Y. Y., Kim, S.-W., Gentner, D. R., Isaacman-VanWertz, G., Goldstein, A. H., Harley, R. A., Frost, G. J., Roberts, J. M., Ryerson, T. B., and Trainer, M.: Volatile chemical products emerging as largest petrochemical source of urban organic emissions, Science, 359, 760–764, https://doi.org/10.1126/science.aaq0524, 2018.

Mo, Z., Shao, M., Liu, Y., Xiang, Y., Wang, M., Lu, S., Ou, J., Zheng, J., Li, M., Zhang, Q., et al.: Species-specified VOC emissions derived from a gridded study in the Pearl River Delta, China, Scientific Reports, 8, 2963, https://doi.org/10.1038/s41598-018-21296-y, 2018.

Yan, L., Zheng, B., Geng, G., Hong, C., Tong, D., and Zhang, Q.: Evaporation process dominates vehicular NMVOC emissions in China with enlarged contribution from 1990 to 2016, Environmental Research Letters, 16, 124 036, https://doi.org/10.1088/1748-9326/ac3872, 2021.

Cai, Z., Xie, Q., Yang, L., Yuan, B., Wu, G., Zhu, Z., Wu, L., Chang, M., & Wang, X. (2023). A novel method for spatial allocation of volatile chemical products emissions: A case study of the Pearl River Delta. Atmospheric Environment, 314, 120119.